Received: 2 August 2022 | Revised: 23 October 2022 | Accepted: 18 November 2022

DOI: 10.1002/glia.24312

GLIA

WILEY

RESEARCH ARTICLE

Altered glial expression of the cannabinoid 1 receptor in the subiculum of a mouse model of Alzheimer's disease

Itziar Terradillos[1,2] | Itziar Bonilla-Del Río[1,2] | Nagore Puente[1,2] | Maitane Serrano[1,2] | Amaia Mimenza[1,2] | Leire Lekunberri[1,2] | Ilazki Anaut-Lusar[1,2] | Leire Reguero[1,2] | Inmaculada Gerrikagoitia[1,2] | Samuel Ruiz de Martín Esteban[3] | Cecilia J. Hillard[4] | María T. Grande[3] | Julián Romero[3] | Izaskun Elezgarai[1,2] | Pedro Grandes[1,2]

[1]Department of Neurosciences, Faculty of Medicine and Nursing, University of the Basque Country UPV/EHU, Leioa, Spain

[2]Achucarro Basque Center for Neuroscience, Leioa, Spain

[3]Faculty of Experimental Sciences, Universidad Francisco de Vitoria, Pozuelo de Alarcón, Spain

[4]Department of Pharmacology and Toxicology, Neuroscience Research Center, Medical College of Wisconsin, Milwaukee, Wisconsin, USA

Correspondence
Pedro Grandes, Department of Neurosciences, Faculty of Medicine and Nursing, University of the Basque Country UPV/EHU, Leioa, Spain.
Email: pedro.grandes@ehu.eus

Funding information
Eusko Jaurlaritza, Grant/Award Numbers: IT1230-19, IT1620-22; Ministerio de Ciencia e Innovación, Grant/Award Numbers: PID2019-107548RB-I00, PID2019-108992RB-I00; Research and Education Component of the Advancing a Healthier Wisconsin Endowment at the Medical College of Wisconsin

Abstract

The alteration of the endocannabinoid tone usually associates with changes in the expression and/or function of the cannabinoid CB_1 receptor. In Alzheimer's disease (AD), amyloid beta (Aβ)-containing aggregates induce a chronic inflammatory response leading to reactivity of both microglia and astrocytes. However, how this glial response impacts on the glial CB_1 receptor expression in the subiculum of a mouse model of AD, a brain region particularly affected by large accumulation of plaques and concomitant subcellular changes in microglia and astrocytes, is unknown. The CB_1 receptor localization in both glial cells was investigated in the subiculum of male 5xFAD/$CB_2^{EGFP/f/f}$ (AD model) and $CB_2^{EGFP/f/f}$ mice by immuno-electron microscopy. The findings revealed that glial CB_1 receptors suffer remarkable changes in the AD mouse. Thus, CB_1 receptor expression increases in reactive microglia in 5xFAD/$CB_2^{EGFP/f/f}$, but remains constant in astrocytes with CB_1 receptor labeling rising proportionally to the perimeter of the reactive astrocytes. Not least, the CB_1 receptor localization in microglial processes in the subiculum of controls and closely surrounding amyloid plaques and dystrophic neurites of the AD model, supports previous suggestions of the presence of the CB_1 receptor in microglia. These findings on the correlation between glial reactivity and the CB_1 receptor expression in microglial cells and astrocytes, contribute to the understanding of the role of the endocannabinoid system in the pathophysiology of Alzheimer's disease.

KEYWORDS
astroglia, endocannabinoid system, immuno-electron microscopy, microglia, neurodegeneration

Itziar Terradillos and Itziar Bonilla-Del Río share first authorship.

1 | INTRODUCTION

Astrocytes and microglia activity associated with chronic inflammation induced by Aβ-containing aggregates results in abnormal morphology and proliferation of both glial cells in AD (Benito et al., 2003; McAlpine et al., 2021; Smit et al., 2021). The potential of cannabinoids to target several processes involved in AD pathogenesis is regarded as a therapeutic strategy (Casarejos et al., 2013; Chen et al., 2012; Eljaschewitsch et al., 2006; Talarico et al., 2019), in part because the main cannabinoid CB_1 receptor is localized in brain regions and cells, including glia, affected by the disease. We have previously estimated that about 56% of the CB_1 receptor labeling localizes to GABAergic terminals, 12% to glutamatergic terminals, 6% to astrocytes, 15% to mitochondria and the rest to other cells and compartments to be determined (Bonilla-Del Río et al., 2019; Bonilla-Del Río et al., 2021).

The expression of CB_1 receptors in astrocytes seems to be regulated by multiple factors and can vary under different brain conditions, for example, transient receptor potential vanilloid 1 knock out mice show a significant decrease in CB_1 density in astrocytes (Egaña-Huguet et al., 2021), acute Δ-9-tetrahydrocannabinol exposure causes CB_1 increase in these glial cells (Bonilla-Del Río et al., 2021), or adolescent binge drinking significantly decreases CB_1 in astrocytes in the adult brain (Bonilla-Del Río et al., 2019). Although the impact that astroglial dysfunction may have in AD is still poorly understood (Smit et al., 2021; Verkhratsky & Nedergaard, 2018), pieces of evidence suggest that changes in the endocannabinoid system occur in astrocytes near AD lesions. Thus, astrocytes closely associated with Aβ aggregates show more intermediate filament proteins and hypertrophy of cell bodies (Escartin et al., 2019; Smit et al., 2021). These astrocytes clear as well as degrade Aβ aggregates and release pro-inflammatory molecules (Farina et al., 2007) which can be diminished by endocannabinoids acting on CB_1 receptors localized in these glial cells (Metna-Laurent & Marsicano, 2015). Also, high fatty acid amide hydrolase (FAAH) levels, the main degrading enzyme for the endocannabinoid anandamide, have been found in astrocytes around neuritic plaques (Abate et al., 2021; Benito et al., 2003). However, the real impact of the progression of Alzheimer's disease on the expression of CB_1 receptors in astrocytes surrounding the lesions is unknown.

Microglia is another important player in the pathogenesis of Alzheimer's disease. Cannabinoids prevent Aβ-induced neurodegeneration by reducing microglial activity. Both CB_1 and CB_2 receptors expressed in microglia are involved in this action as they inhibit neuroinflammation by preventing reactive oxygen species (ROS) formation and cytokines release by these cells (Casarejos et al., 2013; Martín-Moreno et al., 2011; Ramírez et al., 2005; Talarico et al., 2019). Microglia also elicits a significant increase in endocannabinoid production that, in turn, activates more CB_1 and CB_2 receptors and their signaling cascades, amplifying the anti-inflammatory and protective microglial phenotype (Duffy et al., 2021; Mecha et al., 2016). In fact, the number and Aβ phagocytic capacity of microglial cells decrease in mice lacking CB_2 receptors (de Martín et al., 2022).

There are pieces of evidence indicating that microglia constitutively expresses CB_1 receptors that mediate some of the cannabinoid effects in resting microglial cells (Kaplan, 2013; Navarro et al., 2018; Ribeiro et al., 2013; Stella, 2009; Thion et al., 2018), and regulate neuroinflammation in a sex-dependent manner (De Meij et al., 2021). CB_1 receptors have been noticed in cultured microglia (Carlisle et al., 2002; Facchinetti et al., 2003; Klegeris et al., 2003; Molina-Holgado et al., 2002; Sinha et al., 1998; Stefano et al., 1996; Waksman et al., 1999; Walter et al., 2003), and specific anti-CB_1 antibodies detected some scattered CB_1 signal in microglia in the hypothalamic arcuate nucleus of females (De Meij et al., 2021).

CB_1 receptor expression increases in many inflammatory and neurodegenerative diseases like AD (Bisogno & Di Marzo, 2010; Ribeiro et al., 2013); however, very little is known about the localization and expression of cannabinoid receptors in glial cells in AD. We hypothesize in this study that CB_1 receptor expression in glia is altered in the subiculum of a mouse model of AD, a brain region particularly affected by large accumulation of plaques, as a result of concomitant subcellular changes in microglia and astrocytes. Our findings show that CB_1 receptors in microglial cells suffer remarkable modifications in 5xFAD/$CB_2^{EGFP/f/f}$ mice, a murine model of AD recently reported to have an increase in CB_2 receptors in microglia related to dystrophic neurites (Ruiz de Martín Esteban et al., 2022), similarly to the CB_2 rise observed in plaque-associated microglia (Benito et al., 2003, 2007).

2 | MATERIAL AND METHODS

2.1 | Ethics statement

The protocols for animal care and use were approved by the Committee of Ethics for Animal Welfare of the University of the Basque Country (M20/2020/109) and were in accordance to the European Communities Council Directive of September 22, 2010 (2010/63/EU) and Spanish regulations (Real Decreto 53/2013, BOE 08-02-2013). Efforts were made to minimize the number and suffering of animals.

2.2 | Experimental animals

Experiments were done in 6.5–7.5-month-old male $CB_2^{EGFP/f/f}$ mice, controls and co-expressing five AD mutations (5xFAD; Oakley et al., 2006) previously used in our laboratory for the localization of CB_2 receptors (Ruiz de Martín Esteban et al., 2022). The $CB_2^{EGFP/f/f}$ mice were generated at the Genoway facilities (Lyon, France) by designing a targeting strategy consisting of the insertion of an enhanced green fluorescent protein (EGFP) reporter gene, preceded by an internal ribosomal entry site sequence (IRES) into the 3′ untranslated region (UTR) of the mouse cnr2 gene. This resulted in expression of the reporter gene (EGFP) under the control of the

mouse endogenous cnr2 promoter, and transcription of the same bicistronic mRNA as the CB_2 receptor protein. In addition, these mice co-expressed 5xFAD mutations at the same time. The 5xFAD mice with a C57BL/6J background were purchased from Jackson Laboratory (Bar Harbor, Main, USA). To obtain the co-expression, 5xFAD mice were mated with $CB_2^{EGFP/f/f}$ mice for at least five generations to generate 5xFAD/$CB_2^{EGFP/f/f}$ mice (López et al., 2018). This 5xFAD model does not seem to express the mutation that causes the neurofibrillary degeneration (Oblak et al., 2021), but it may occur indirectly through neuronal degeneration and Aβ 1–42 deposits.

2.3 | Brain tissue processing

Mice were anesthetized with ketamine/xylazine (100 mg/10 mg/kg body weight, intraperitoneal injection) and subsequently perfused transcardially at room temperature (RT) through the left ventricle. First with phosphate buffered saline (PBS) 0.1 M (pH 7.4) for 20 s, and then with the fixative solution composed of 4% formaldehyde, 0.2% picric acid and 0.1% glutaraldehyde in PBS 0.1 M (pH 7.4) for 10–15 min, with a fixative solution volume of 80 ml per mouse. The brains were then removed from the skull and post-fixed in the fixative solution for approximately 1 week at 4°C. Subsequently, they were stored in 1:10 diluted fixative solution at 4°C with 0.025% sodium azide. Brain vibrosections were cut coronally at 50 μm and stored with 1 ml of phosphate buffer (PB) 0.1 M (pH 7.4) with 0.025% sodium azide at 4°C.

2.4 | Immunohistochemistry for light microscopy

Brain sections containing the subiculum were collected in PB 0.1 M (pH 7.4) at RT, pre-incubated with a blocking solution of 10% bovine serum albumin (BSA), 0.1% sodium azide and 0.5% triton X-100 in 1x tris-buffered saline (TBS 1x) (pH 7.4) for 30 min at RT, and incubated with the following primary polyclonal antibodies: guinea pig anti-CB_1 receptor (1:100; CB_1-GP-Af530; AB_2571593, Frontier Institute Co., ltd), rabbit anti-ionized calcium-binding adapter molecule 1 (Iba1, 1:500; 019-19741; AB_839504, FUJIFILM Wako Pure Chemical Corporation), rabbit anti-glutamate aspartate transporter 1 (Anti-A522 [GLAST] EAAT1, 0.3 μg/ml; Ab#314; AB_231456, kindly gifted by Prof. Niels Christian Danbolt, University of Oslo). They were prepared in blocking solution and gently shaken for 2 days at 4°C or 1 day at RT. Then, sections were washed with 1% BSA and 0.5% triton X-100 in TBS 1x for 30 min, and incubated with a biotinylated anti-guinea pig (1:200, Biotin-SP-AffiniPure Goat Anti-Guinea Pig IgG; AB_2337394, Jackson Immuno Research), or biotinylated anti-rabbit secondary antibody (1:200, Biotin-SP-AffiniPure Donkey Anti-Rabbit IgG; AB_2340593, Jackson Immuno Research) diluted in the washing solution for 1 h on a shaker at RT. They were washed with 1% BSA and 0.5% triton X-100 in TBS 1x (30 min). Tissue was incubated with the avidin-biotin peroxidase complex (ABC; 1:50, Elite, Vector Laboratories, Burlingame, CA, USA) prepared in the washing solution, for 1 h at RT. Samples were washed with 1% BSA and 0.5% triton X-100 in TBS 1x (3 x 1 min) and lastly with PB 0.1 M (pH 7.4) and 0.5% triton X-100 (2 x 10 min). Labeling was revealed with 0.05% diaminobenzidine (DAB) in PB 0.1 M (pH 7.4) containing 0.5% triton X-100 and 0.01% hydrogen peroxide for 3.5 min at RT. This was followed by washes in PB 0.1 M (pH 7.4) with 0.5% triton X-100 (3 x 1 min, 2 x 10 min). Tissue sections were mounted on gelatinized slides, dried and dehydrated in graded ethanol for 5 min each. After rinsing with xylene (3 x 5 min), the slides were cover slipped with DPX. The subiculum was examined and photographed with a Zeiss AxioCam light microscope coupled to a Zeiss AxioCam HRc camera.

2.5 | Immunohistochemistry for electron microscopy

The protocol is already published (Puente et al., 2019). Four to five sections per brain containing the subiculum were selected. They were pre-incubated in a blocking solution (1 ml/well) of 10% BSA, 0.02% saponin and 0.1% sodium azide in TBS 1x (pH 7.4), for 30 min on the shaker at RT. Tissue was then incubated with a primary guinea pig anti-CB_1 receptor antibody (1:100) in combination with a rabbit anti-GLAST antibody (0.3 μg/ml) or a rabbit anti-Iba1 antibody (1:500). The solution contained 10% BSA in TBS 1x, 0.1% sodium azide and 0.004% saponin. Incubation was performed on a shaker for 2 days at 4°C followed by washes in 1% BSA/TBS 1x. Then, sections were incubated with 1.4 nm gold-conjugated goat anti-guinea pig IgG antibody (Fab fragment, 1:100, #2055, Nanoprobes, Inc., Yaphank, NY, USA). They were also incubated with biotinylated anti-rabbit IgG antibody (1:200) diluted in 1% BSA/TBS 1x with 0.004% saponin on a shaker for 4 h at RT. Tissue was washed in 1% BSA/TBS 1x on a shaker at RT and incubated with ABC (1:50) prepared in washing solution for 1.5 h at RT. Sections were washed in 1% BSA/TBS 1x, kept overnight at 4°C and post-fixed with 1% glutaraldehyde in TBS 1x (1 ml/well) for 12 min at RT. Then, they were washed in double distilled water and gold particles were silver-intensified with the HQ Silver kit (#2012, Nanoprobes, Inc., Yaphank, NY, USA) in the dark for 12 min at RT. After intensification, the sections were washed first in double distilled water and then with PB 0.1 M (pH 7.4) for 30 min. The biotinylated antibody was revealed with 0.05% DAB prepared in PB 0.1 M (pH 7.4) containing 0.5% triton X-100 and 0.01% hydrogen peroxide for 3.5 min at RT, followed by several washes in PB 0.1 M (pH 7.4). They were osmicated (1% osmium tetroxide in PB 0.1 M, pH 7.4) in the dark for 20 min, washed in PB 0.1 M (pH 7.4), dehydrated in graded ethanol, cleared in propylene oxide, pre-embedded in 1:1 propylene oxide/Epon 812 resin on a shaker overnight at RT and embedded in pure Epon 812 resin. Immunogold labeling was visualized with a light microscope in sections containing the subiculum, and tissue portions with good and consistent CB_1 receptor labeling were identified and trimmed down for ultrathin sectioning. The procedure has already been described in detail (Bonilla-Del Río et al., 2019; Bonilla-Del Río et al., 2021; Gutiérrez-Rodríguez et al., 2018; Puente et al., 2019). Three to four semi-thin sections (0.7 μm-thick) were obtained with a histo-diamond knife (Diatome USA) and stained with 1% toluidine blue. To further standardize the conditions, only the

first five ultrathin sections were cut (50 nm-thick) with an ultra-diamond knife (Diatome USA), collected onto nickel mesh grids and counterstained with 2.5% lead citrate for 20 min at RT. Electron micrographs were randomly taken with a Hamamatsu FLASH digital camera inserted in a transmission electron microscope (JEOL JEM 1400 Plus). Sampling was always carefully and accurately done using the following anatomical coordinates to delimit the subiculum: interaural, 0.40/0.00 mm; bregma, −3.40/−3.80 mm (Franklin & Paxinos, 2008).

2.6 | Antibodies specificity

Experiments were always performed under the same conditions. In addition, negative controls omitting the primary antibodies were done. Furthermore, the CB_1 receptor antibody was tested in CB_1−/− brain tissue (Marsicano et al., 2002) by double pre-embedding immunogold (CB_1) and immunoperoxidase (Iba1 or GLAST) method for electron microscopy (Figure 1). The anti-A522 (EAAT1 [GLAST]) antibody (Ab#314) targeting the C-terminal residues 522–541 of rat EAAT1 (Hu et al., 2020) was used to identify astrocytic compartments. GLAST was restricted to astrocytes and localized intracellularly with no detectable labeling in nerve terminals, as previously described (Lehre et al., 1995; Schmitt et al., 1997). Furthermore, GLAST distribution is very similar in rodents and humans (Li et al., 2012), so the use of anti-GLAST antibody is a good approach to label astrocytes in the AD model. The specificity of the Iba1 antibody has been confirmed in previous studies (Delcambre et al., 2016; Szabo & Gulya, 2013). GLAST can be expressed in both microglia and astrocytes under certain conditions (Beschorner et al., 2007). Experiments were conducted to figure this out. Strikingly, GLAST and Iba1 were not seen to co-localize in a subicular area of 3506 μm^2 analyzed in $CB_2^{EGFP/f/f}$ and of 4743 μm^2 in 5xFAD/$CB_2^{EGFP/f/f}$ (data not shown). Taken together, we could reasonably conclude that GLAST and Iba1 are selective markers for astrocyte and microglia, respectively, in the 6.5–7.5 month-old-$CB_2^{EGFP/f/f}$ and 5xFAD/$CB_2^{EGFP/f/f}$ mice studied.

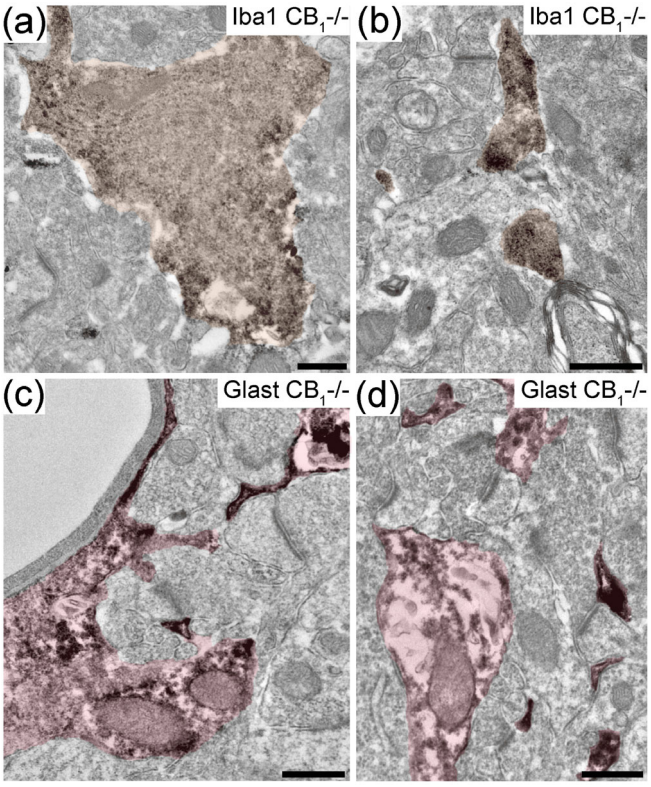

FIGURE 1 Subiculum of CB_1 knock out mice (CB_1−/−). Double immunogold and immunoperoxidase method for electron microscopy. Antibodies were tested in CB_1−/− mice (a–d). Simultaneous labeling for CB_1 (gold) and Iba1 (a and b; DAB immunodeposits in brown) or GLAST (c and d; DAB in pink). No CB_1 receptor signal is observed. Scale bars: 50 nm

2.7 | Quantitative and statistical assessment

To ensure homogeneous labeling between all samples, only the first 1.5 μm from the section surface of each specimen were considered for the analysis. Area, perimeter, number of processes and CB_1 receptor expression in astrocytes, were studied in 5596 μm^2 of five $CB_2^{EGFP/f/f}$, and in 7681 μm^2 of seven 5xFAD/$CB_2^{EGFP/f/f}$ mice. In addition, the area, perimeter and number of microglial processes were measured in 7900 μm^2 of seven $CB_2^{EGFP/f/f}$, and in 10,793 μm^2 of 10 5xFAD/$CB_2^{EGFP/f/f}$ mice. For the study of CB_1 receptors in microglia, 6345 μm^2 in five $CB_2^{EGFP/f/f}$ and 7268 μm^2 in seven 5xFAD/$CB_2^{EGFP/f/f}$ mice, were analyzed.

CB_1 receptor labeling in astrocytes and microglia was assessed in GLAST- and Iba1-immunopositive processes, respectively. The proportion of cell compartments with CB_1 receptor signal was then tabulated. Positive labeling was considered when at least one immunoparticle was within 30 nm of the membrane studied. CB_1 receptor density (particles/μm membrane) was also determined by counting gold particles in the positive compartments. Membrane length (perimeter) was measured with the Image-J software (NIH; SCR_003070).

All values were given as mean ± S.E.M. using a statistical software package (GraphPad Prism 8, SCR_002798, GraphPad Software, Inc., San Diego, USA). The normality test (Kolmogorov–Smirnov normality test) was always applied before statistics was done. Data were analyzed by non-parametric or parametric tests: Mann–Whitney U test or Student's Unpaired t-test (*$p < .05$).

Minor contrast and brightness adjustments were made to the figures using Adobe Photoshop (Adobe Photoshop, SCR_014199, CS3, Adobe Systems, San Jose, CA, USA) and Gimp (GNU Image Manipulation Program, SCR_003182).

3 | RESULTS

3.1 | Glial morphology in the subiculum of $CB_2^{EGFP/f/f}$ and 5xFAD/$CB_2^{EGFP/f/f}$ mice

Changes in staining density were detected in microglial and astrocytic cells (Figure 2a–d). Microglia identified by Iba1 in $CB_2^{EGFP/f/f}$

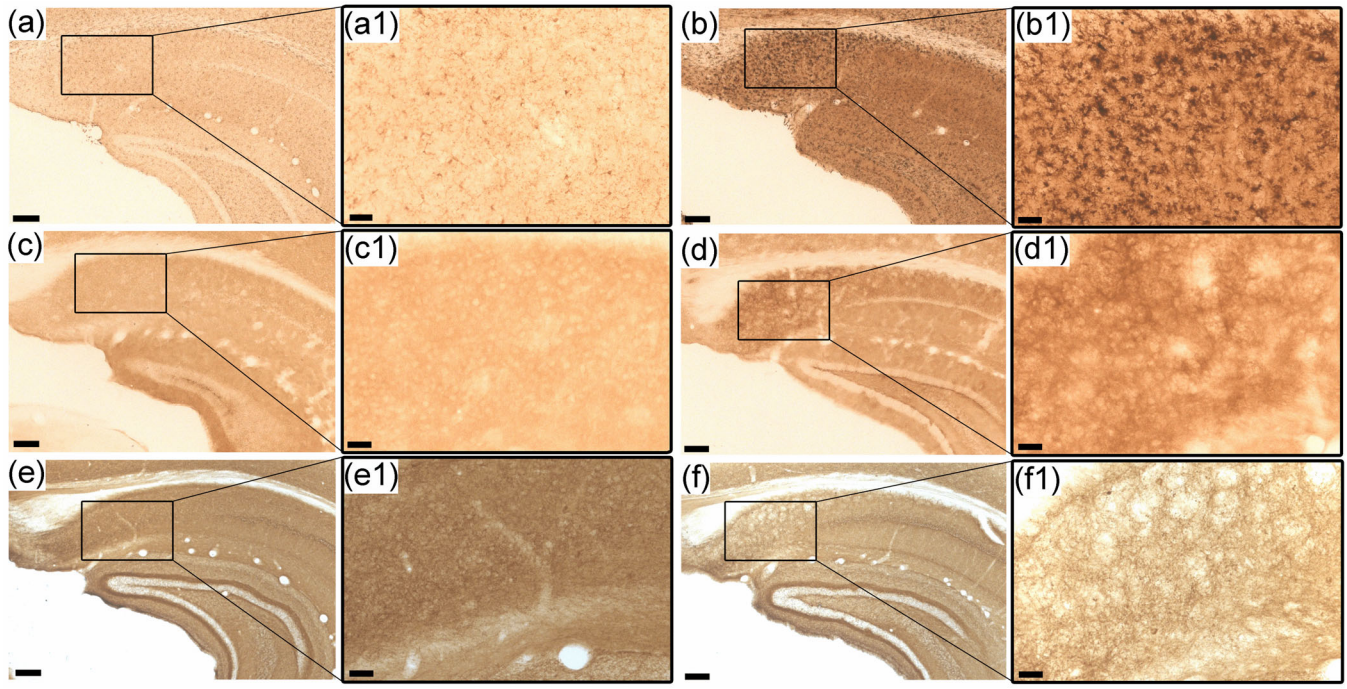

FIGURE 2 Subiculum of $CB_2^{EGFP/f/f}$ and 5xFAD/$CB_2^{EGFP/f/f}$ mice showing Iba1, GLAST and CB_1 immunostaining. Avidin-biotin peroxidase method for light microscopy. Iba1 in $CB_2^{EGFP/f/f}$ (a, a1) is drastically increased in 5xFAD/$CB_2^{EGFP/f/f}$ microglia (b, b1). GLAST in $CB_2^{EGFP/f/f}$ (c, c1) is weaker than in 5xFAD/$CB_2^{EGFP/f/f}$ (d, d1). Dense CB_1 receptor staining in $CB_2^{EGFP/f/f}$ (e, e1) changes to a weaker and more patchy appearance in 5xFAD/$CB_2^{EGFP/f/f}$ (f, f1). Scale bars: 200 μm (a–f) and 50 μm (a1–f1)

(Figure 2a,a1) occupied a much larger area in 5xFAD/$CB_2^{EGFP/f/f}$ (Figure 2b,b1). This increase seemed to relate to both the number of microglial cells and the thickness of their processes (Figure 2a1,b1). In the electron microscope, only scattered microglial processes were observed in controls (Figure 3a,b), while numerous Iba1-positive processes surrounding plaques (Figure 3c,f) and dystrophic neurites (Figure 3c1,c3-f) were seen in 5xFAD/$CB_2^{EGFP/f/f}$ mice. The area of the microglial processes was significantly increased in 5xFAD/$CB_2^{EGFP/f/f}$ (0.3229 ± 0.05282 μm^2; ***$p < .0001$) relative to $CB_2^{EGFP/f/f}$ (0.1000 ± 0.01754 μm^2; Figure 5a), as it was the total microglial area per sample normalized to 100 μm^2 (5xFAD/$CB_2^{EGFP/f/f}$: 2.074 ± 0.5156 μm^2; ***$p < .0001$; $CB_2^{EGFP/f/f}$: 0.3485 ± 0.06955 μm^2; Figure 5b). In addition, a significant increase in the perimeter of the microglial prolongations was detected in 5xFAD/$CB_2^{EGFP/f/f}$ (2.200 ± 0.1248 μm; ***$p < .0001$) versus $CB_2^{EGFP/f/f}$ (1.260 ± 0.1036 μm; Figure 5c) and reflected in the perimeter of the total microglial processes per sample normalized to 100 μm^2 (15.73 ± 1.929 μm in 5xFAD/$CB_2^{EGFP/f/f}$; 4.334 ± 0.5345 μm in $CB_2^{EGFP/f/f}$; ***$p < .0001$; Figure 5d). Finally, significant changes were also noticed in the number of microglial processes (7.260 ± 0.6304/100 μm^2 in 5xFAD/$CB_2^{EGFP/f/f}$; 3.413 ± 0.4092/100 μm^2 in $CB_2^{EGFP/f/f}$; ***$p < .0001$; Figure 5e).

As to astrocytes, GLAST staining seen in $CB_2^{EGFP/f/f}$ (Figure 2c,c1) was more intense in 5xFAD/$CB_2^{EGFP/f/f}$ (Figure 2d,d1). By using GLAST-DAB, the area, perimeter and number of astrocytic elements were analyzed in the electron microscope (Figure 4). Astrocytic processes surrounded dystrophic neurites and plaques in 5xFAD/$CB_2^{EGFP/f/f}$ (Figure 4b–d) and showed a significant increase in their area (5xFAD/$CB_2^{EGFP/f/f}$: 0.2598 ± 0.01853 μm^2; $CB_2^{EGFP/f/f}$: 0.1565 ± 0.006515 μm^2; ***$p < .0001$; Figure 5a). However, no differences were observed in the total area per sample occupied by astrocytic processes normalized to 100 μm^2 (5xFAD/$CB2^{EGFP/f/f}$: 8.993 ± 0.8664 μm^2; $CB2^{EGFP/f/f}$: 7.415 ± 0.6552 μm^2; p: .1711; Figure 5b). There was also a great increase in the perimeter of the astrocytic processes (5xFAD/$CB_2^{EGFP/f/f}$: 2.833 ± 0.08486 μm; $CB_2^{EGFP/f/f}$: 2.116 ± 0.04741 μm; ***$p < .0001$; Figure 5c). Nevertheless, no differences in the total perimeter of astrocytic processes per sample were detected (5xFAD/$CB_2^{EGFP/f/f}$: 99.89 ± 8.087 μm; $CB_2^{EGFP/f/f}$: 100.1 ± 6.811 μm; p: .9820; Figure 5d). Consistent with these results, a significant decrease in the number of astrocytic processes in 5xFAD/$CB_2^{EGFP/f/f}$ (35.52 ± 2.661 per 100 μm^2) relative to $CB_2^{EGFP/f/f}$ (47.33 ± 2.709 per 100 μm^2) was noticed (**p: .0036; Figure 5e).

Overall, our analyses in the subiculum of the Alzheimer's model reveal that the larger area of the microglia correlates with an increase in size and number of their processes, while astrocytic projections are fewer but bigger (Figure 5a–e).

3.2 | CB_1 receptors in $CB_2^{EGFP/f/f}$ and 5XFAD/$CB_2^{EGFP/f/f}$ subiculum

The CB_1 receptor labeling observed in $CB_2^{EGFP/f/f}$ (Figure 2e,e1) was more patchy in 5xFAD/$CB_2^{EGFP/f/f}$ showing many delimited round areas with much lower or insignificant staining, probably corresponding to neuritic plaques surrounded by a neuropil with more CB_1 receptor immunoreactivity (Figure 2f,f1).

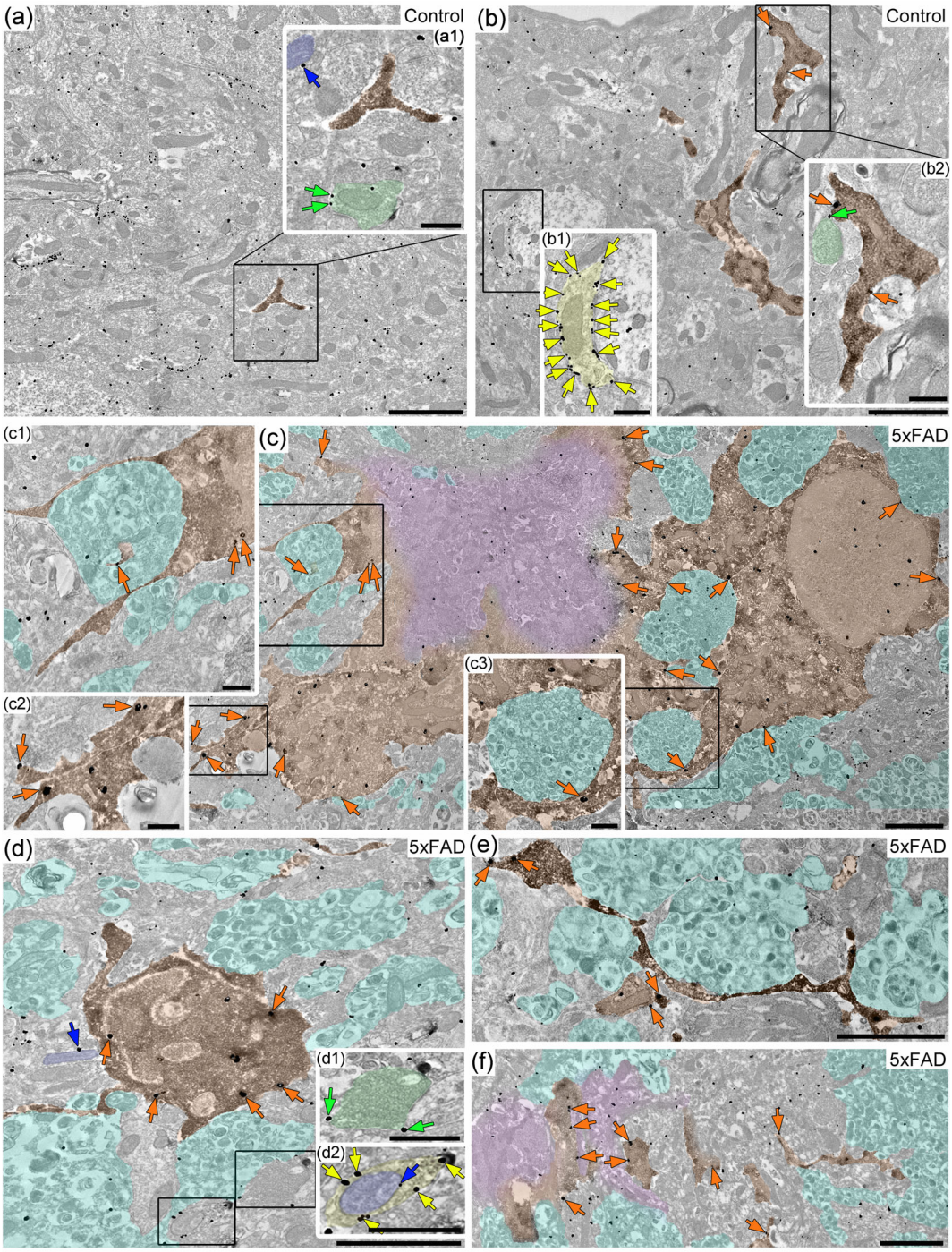

FIGURE 3 Double pre-embedding immunogold (CB_1) and immunoperoxidase (Iba1) method for electron microscopy in the subiculum of $CB_2^{EGFP/f/f}$ and 5xFAD/$CB_2^{EGFP/f/f}$ mice. In $CB_2^{EGFP/f/f}$, a few slender Iba1 positive microglial elements are observed (a, b) (DAB immunodeposits in brown). However, thick processes of reactive microglia appear in 5xFAD/$CB_2^{EGFP/f/f}$ (c–f) surrounding plaques (in purple; c, f) and dystrophic neurites (in turquoise; c–f). Notice membrane CB_1 particles (orange arrows) in microglial processes of $CB_2^{EGFP/f/f}$ (b2) and 5xFAD/$CB_2^{EGFP/f/f}$ (c–f), with particular abundance in 5xFAD/$CB_2^{EGFP/f/f}$. CB_1 receptor labeling is also in membranes of excitatory terminals (green arrows and profiles in a1, b2 and d1), inhibitory terminals (yellow arrows and profiles in b1, d2) and mitochondria (blue arrows and profiles in a1 and d2), in both mutants. Scale bars: 2 μm

3.3 | Microglial CB_1 receptor localization in $CB_2^{EGFP/f/f}$ and 5XFAD/$CB_2^{EGFP/f/f}$ subiculum

CB_1 receptor particles were localized to membranes of Iba1-positive microglial processes in both $CB_2^{EGFP/f/f}$ (Figure 3b2) and 5xFAD/$CB_2^{EGFP/f/f}$ mice (Figure 3c–f). The analysis revealed a significant increase in CB_1-positive microglial processes in 5xFAD/$CB_2^{EGFP/f/f}$ (0.9942 ± 0.1259 CB_1^+ processes/100 μm^2) compared to $CB_2^{EGFP/f/f}$ (0.3254 ± 0.07758 CB_1^+ processes/100 μm^2; ***p < .0001; Figure 6a, left). In addition, a strike increase in the proportion of CB_1-positive

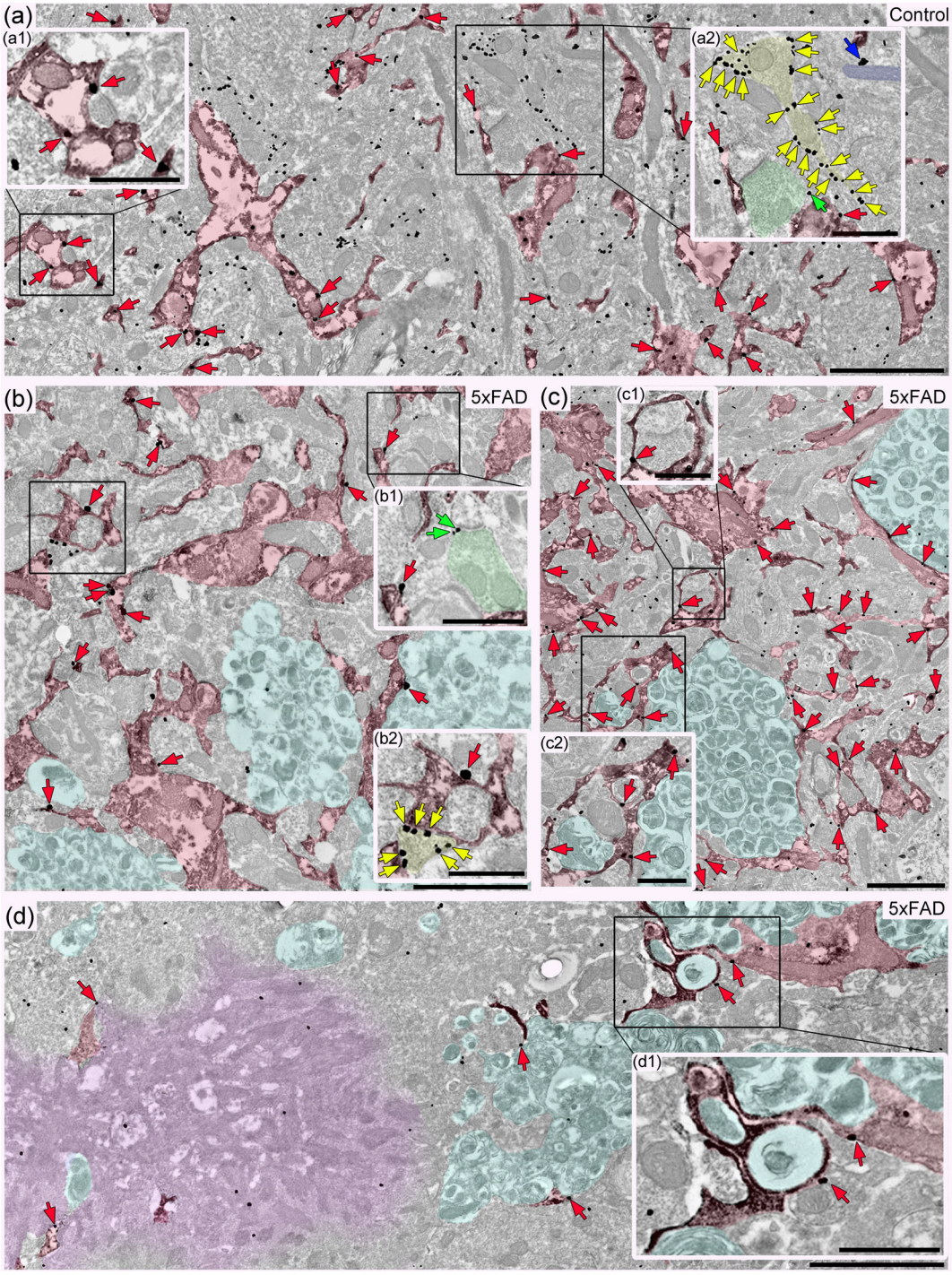

FIGURE 4 Double pre-embedding immunogold (CB_1 receptor) and immunoperoxidase (GLAST) method for electron microscopy in the subiculum of $CB_2^{EGFP/f/f}$ and 5xFAD/$CB_2^{EGFP/f/f}$ mice. GLAST-positive astrocytic processes (DAB immunodeposits in pink) seen in $CB_2^{EGFP/f/f}$ (a) are thicker in 5xFAD/$CB_2^{EGFP/f/f}$ (b–d). Observe astrocytic elements surrounding dystrophic neurites (turquoise in b–d) and close to a plaque (purple in d) in the 5xFAD/$CB_2^{EGFP/f/f}$. CB_1 particles (red arrows) localize to plasma membranes of GLAST-positive astrocytic processes in $CB_2^{EGFP/f/f}$ (a) and 5xFAD/$CB_2^{EGFP/f/f}$ (b–d). Typical CB_1 receptor labeling is also observed in membranes of excitatory terminals (green arrows and profiles in a2, b1), inhibitory terminals (yellow arrows and profiles in a2, b2) and mitochondria (blue arrows and profiles in a2), in both $CB_2^{EGFP/f/f}$ and 5xFAD/$CB_2^{EGFP/f/f}$. Scale bars: 2 μm

elements was detected in 5xFAD/$CB_2^{EGFP/f/f}$ mice (6.27 ± 1.15%; $CB_2^{EGFP/f/f}$: 3.79 ± 2.10%; ***p*: .0033; Figure 6b, left). However, CB_1 receptor density in the positive microglial processes was significantly reduced in 5xFAD/$CB_2^{EGFP/f/f}$ (69.44 ± 7577 particles/100 μm of membrane; $CB_2^{EGFP/f/f}$: 135.5 ± 24.78/100 μm of membrane; ***p*: .0023; Figure 6c, left). Furthermore, significant differences in the total number of microglial CB_1 particles per 100 μm^2 were observed between 5xFAD/$CB_2^{EGFP/f/f}$ (1.31 ± 0.18 particles) and $CB_2^{EGFP/f/f}$

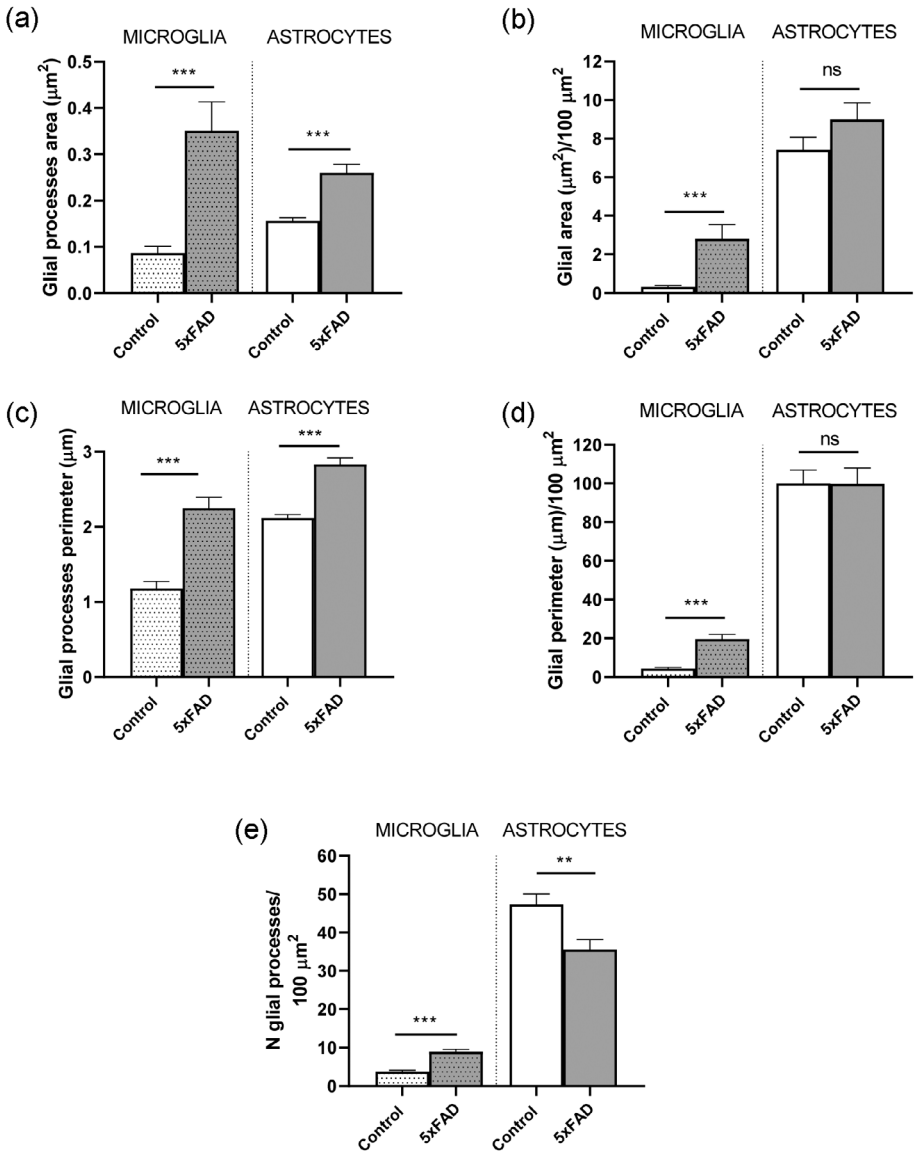

FIGURE 5 Morphological parameters of microglia and astrocytes in the subiculum of $CB_2^{EGFP/f/f}$ and 5xFAD/$CB_2^{EGFP/f/f}$ mice. (a) Microglial and astrocytic processes area. (b) Glial area (microglia and astrocytes) normalized to 100 μm^2. (c) Microglial and astrocytic processes perimeter. (d) Glial perimeter (microglia and astrocytes) normalized to 100 μm^2. (e) Number of glial processes (microglia and astrocytes) in 100 μm^2. Data were analyzed by non-parametric or parametric tests (Mann–Whitney *U*-test or Student's *t*-test). Mann–Whitney *U*-test or Student's *t*-test. $p < .05$*; $p < .01$**; $p < .001$***; $p < .0001$****. All data are represented as mean ± SEM

(0.48 ± 0.13 particles; ***p: .0009; Figure 6d, left). Finally, there were not differences in the number of CB_1 particles per positive microglial process between both mutants (5xFAD/$CB_2^{EGFP/f/f}$: 1.333 ± 0.08347 particles/process; $CB_2^{EGFP/f/f}$: 1.450 ± 0.2112 particles/process; p: .7736; Figure 6e, left).

3.4 | Astroglial CB_1 receptor localization in $CB_2^{EGFP/f/f}$ and 5XFAD/$CB_2^{EGFP/f/f}$ subiculum

The CB_1 receptor was localized to membranes of GLAST-positive astrocytic processes in both mutants (Figure 4a–d), as previously reported (Bonilla-Del Río et al., 2019; Bonilla-Del Río et al., 2021; Bosier et al., 2013; Gutiérrez-Rodríguez et al., 2018; Han et al., 2012). No significant differences were detected in the number of CB_1-positive astrocytic prolongations between both mice ($CB_2^{EGFP/f/f}$: 8.661 ± 0.8977 CB_1^+ processes/100 μm^2; 5xFAD/$CB_2^{EGFP/f/f}$: 7.967 ± 1.224 CB_1^+ processes/100 μm^2; p: .3094; Figure 6a, right). Likewise, the percentage of CB_1-positive astrocytic branches was statistically similar between 5xFAD/$CB_2^{EGFP/f/f}$ (21.24 ± 2.37%) and $CB_2^{EGFP/f/f}$ (17.75 ± 1.21%; p: .2303; Figure 6b, right). There was neither differences in CB_1 receptor density in the astrocytic positive processes (5xFAD/$CB_2^{EGFP/f/f}$: 29.15 ± 2.220 particles/100 μm of membrane; $CB_2^{EGFP/f/f}$: 37.57 ± 2.970 particles/100 μm of membrane; p: .2209; Figure 6c, right), nor in the number of astrocytic CB_1 particles per 100 μm^2 (5xFAD/$CB_2^{EGFP/f/f}$: 12.78 ± 2.174 particles; $CB_2^{EGFP/f/f}$: 11.63 ± 1.265; p: .6716; Figure 6d, right). However, the number of CB_1 particles per positive astrocytic processes was significantly higher in 5xFAD/$CB_2^{EGFP/f/f}$ (1.603 ± 0.05081 particles/process) than in $CB_2^{EGFP/f/f}$ (1.343 ± 0.03909 particles/process; ***p: .0005; Figure 6e, right).

Altogether, the number of microglial processes expressing CB_1 receptors increases and the larger astrocytic profiles have more CB_1 receptors in the subiculum of the Alzheimer's mouse model (Figure 6a–e).

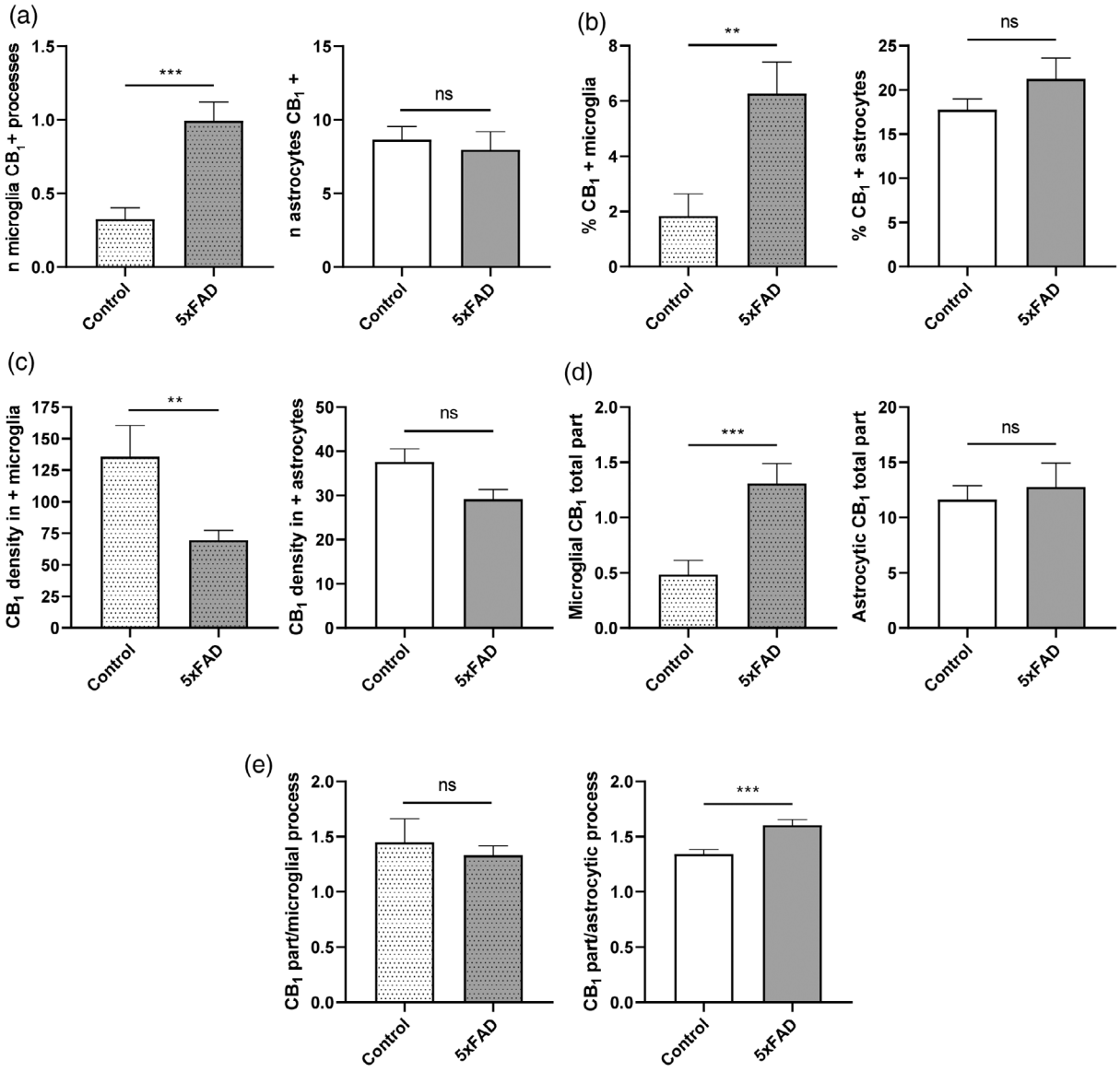

FIGURE 6 Statistical assessment of the CB_1 receptor localization in subicular astrocytes and microglia of $CB_2^{EGFP/f/f}$ and 5xFAD/$CB_2^{EGFP/f/f}$ mice. (a) Number of microglial (left) and astrocytic (right) CB_1 positive processes per 100 μm^2. (b) Percentage of CB_1 positive microglial (left) and astrocytic (right) processes. (c) CB_1 density in positive microglial (left) and astrocytic (right) elements per 100 μm. (d) Microglial (left) and astrocytic (right) CB_1 particles per 100 μm^2. (e) CB_1 receptor labeling per microglial (left) and astrocytic (right) process. Data were analyzed by non-parametric or parametric tests (Mann–Whitney *U*-test or Student's *t*-test). Mann–Whitney *U*-test or Student's *t*-test. $p < .05^*$; $p < .01^{**}$; $p < .001^{***}$; $p < .0001^{****}$. All data are represented as mean ± SEM

4 | DISCUSSION

We detected in the electron microscope the presence of plaques and a multitude of dystrophic neurites in the 5xFAD/$CB_2^{EGFP/f/f}$ mice that confirms the usefulness of this animal model for studying the pathophysiology of AD (Ruiz de Martín Esteban et al., 2022). We also observed an overt microglial and astrocytic reactivity with an increase in the area and perimeter of their processes, demonstrating the existence of significant alterations in the subicular cytoarchitecture. Then we studied the expression of the major cannabinoid CB_1 receptor in glial cells in the subiculum of 5xFAD/$CB_2^{EGFP/f/f}$ and $CB_2^{EGFP/f/f}$ mice. The main findings were that CB_1 receptor expression conspicuously changes in microglial cells but receptor density remains steady in astrocytes despite the reactivity of the astrocytic processes in the AD mouse. Not least, the localization of CB_1 receptors in microglial processes in the subiculum of controls and closely surrounding amyloid plaques and dystrophic neurites in the subiculum of the AD model, supports the presence of CB_1 in microglia. The discreet amount of CB_1 receptors in astrocytes has been revealed accurately by immuno-electron microscopy (Bonilla-Del Río et al., 2021; Gutiérrez-Rodríguez et al., 2018; Puente et al., 2019), a technique that has also been proven in this study to be optimal for the localization of CB_1 receptors in microglia.

4.1 | CB_1 receptors in microglia of $CB_2^{EGFP/f/f}$ and 5XFAD/$CB_2^{EGFP/f/f}$ subiculum

We have shown a very significant increase in the number, area and perimeter of microglial processes in 6.5/7.5-month-old 5xFAD/$CB_2^{EGFP/f/f}$ mice. Proliferation and activity of microglia around amyloid plaques in an attempt to achieve their clearance is a hallmark of AD (Gomez-Nicola & Perry, 2015). Conversely, impaired microglia and altered microglial responses to Aβ are associated with an increased risk of AD (Hansen et al., 2018). In post-mortem samples from AD patients and in murine models of the disease, microgliosis strongly correlates with microglial activity and plaque deposition (Gomez-Nicola & Perry, 2015; Kamphuis et al., 2012; Kettenmann et al., 2011; Olmos-Alonso et al., 2016). The expression of CB_1 receptors in microglia changes depending on the microglial phenotype and profile (Stella, 2010). There are pieces of evidence indicating that microglia constitutively express CB_1 receptors (De Meij et al., 2021; Ribeiro et al., 2013; Stella, 2009) which mediate some of the effects of cannabinoids on these cells (Kaplan, 2013; Navarro et al., 2018). However, microglia hardly express (if any) CB_1 receptors at resting conditions. In fact, specific CB_1 receptor antibodies showed little CB_1 receptor labeling in microglial cells of the female hypothalamic arcuate nucleus (De Meij et al., 2021). Nevertheless, CB_1 receptors have been detected in cultured microglia of several species (Sinha et al., 1998;Stefano et al., 1996; Waksman et al., 1999). We have revealed with the aid of the microglial marker Iba1, the presence of CB_1 receptors in microglial membranes of the $CB_2^{EGFP/f/f}$ subiculum. Furthermore, the number and percentage of CB_1 receptor-positive microglial processes significantly increased in 5xFAD/$CB_2^{EGFP/f/f}$ mice. However, there were not significant changes in the number of CB_1 particles per microglial branch, but a significant decrease in CB_1 receptor density associated with the enlargement of the microglial processes was observed. Interestingly, there were more CB_1 receptor-positive microglial ramifications in 5xFAD/$CB_2^{EGFP/f/f}$.

CB_1 receptor expression increases in many inflammatory and neurodegenerative diseases like AD (Bisogno & Di Marzo, 2010; Ribeiro et al., 2013). However, how CB_1 receptors regulate microglial cell function is still far from being deciphered (Cabral & Marciano-Cabral, 2005; Duncan et al., 2013; Mecha et al., 2015; Steiner et al., 2011). Microglial activity also elicits a significant increase in the endocannabinoids 2-arachydonoyl-glycerol and anandamide that in turn activate cannabinoid receptors and signaling cascades that amplify the anti-inflammatory and protective microglial phenotype (Duffy et al., 2021; Mecha et al., 2016). Thus, microglial CB_1 receptor activation inhibits liposaccharide-induced nitric oxide release (Stefano et al., 1996; Waksman et al., 1999) and MPTP-induced oxidant production (Chung et al., 2011) among other effects (Kaplan, 2013). CB_1 and CB_2 receptors form heteromers with different quaternary structures depending on the microglia state (Navarro et al., 2018). Because CB_2 receptors are selectively expressed in microglia in the vicinity of neuritic plaques and dystrophic neurites (Benito et al., 2003; Bedse et al., 2015; Ruiz de Martín Esteban et al., 2022) and cannabinoids increase CB_1 gene expression through CB_2 (Haspula & Clark, 2020), it is plausible that high levels of CB_2 receptors could affect CB_1 expression near AD lesions. Recent pieces of evidence indicate that CB_1 receptors in mouse microglia promote pro-inflammatory responses in both sexes, but when microglia lack CB_1 receptors a distinct sickness behavior is observed in males subjected to inflammatory conditions (De Meij et al., 2021).

4.2 | CB_1 receptors in astroglia of $CB_2^{EGFP/f/f}$ and 5XFAD/$CB_2^{EGFP/f/f}$ subiculum

Although we observed a significant increase in the number of CB_1 receptor particles per astrocytic process in 5xFAD/$CB_2^{EGFP/f/f}$, there were not significant differences neither in particle number nor in the number or percentage of CB_1-positive processes relative to $CB_2^{EGFP/f/f}$. In addition, CB_1 receptor density was similar between both transgenic mice. However, there was a great increase in the area and perimeter of GLAST-positive astrocytic processes offset by a significant decrease in their number in 5xFAD/$CB_2^{EGFP/f/f}$ mice. That is, there were fewer but larger astrocytic processes in the subiculum of 5xFAD/$CB_2^{EGFP/f/f}$ compared to $CB_2^{EGFP/f/f}$ mice. Therefore, it seems that there were adaptive changes with CB_1 receptors increasing as the reactive astrocytic processes enlarged, keeping unchangeable the density and receptor expression. Altogether, there was a clear astrocytic reactivity around the plaques with not obvious changes in CB_1 receptors.

Astrocytes play an important role in inflammatory processes and their appearance varies through major morphological and molecular changes in the diseased brain (Escartin et al., 2019). For example, astrocytes increase the surface area and reduce the number of processes in the hippocampus of adult mice following ethanol exposure during adolescence (Bonilla-Del Río et al., 2019). Astrocytic swelling leads to astroglial dysfunction and disruption of GFAP found in the astrocyte intermediate filaments (Adermark & Bowers, 2016; Renau-Piqueras et al., 1989). In AD, astroglial reactivity in close association with Aβ aggregates shows a rise in intermediate filament proteins and soma hypertrophy (Escartin et al., 2019; Smit et al., 2021). Astrocytes are able to clear and degrade Aβ aggregates (Bard et al., 2000; Blasko et al., 2004; Wyss-Coray et al., 2003) but also to release pro-inflammatory molecules regulated by astroglial CB_1 receptors (Farina et al., 2007; Metna-Laurent & Marsicano, 2015; Sheng et al., 2005; Stella, 2010). Furthermore, swollen astrocytic processes may not be effective in sensing the endocannabinoids produced on demand by neural activity, and together with high FAAH levels found in astrocytes around neuritic plaques, gliotransmitter availability elicited by cannabinoids could be compromised at the synapses (Abate et al., 2021; Araque et al., 2014; Bedse et al., 2015; Benito et al., 2003; Han et al., 2012). Hence, it is reasonable to expect an impairment in the astroglial anti-inflammatory reaction around plaques and dystrophic neurites in the subiculum of the 5xFAD/$CB_2^{EGFP/f/f}$ mice. In addition, the supposedly resulting disturbance of neurotransmitter clearance and gliotransmission may lead to deficits in synaptic plasticity (Dzyubenko et al., 2016) and, consequently, to brain dysfunction. Astrocytic CB_1 receptors together with the basal endocannabinoid tone play important

roles in brain functions (Navarrete & Araque, 2008, 2010). Also, CB_1 receptors in astrocytes mediate the spatial working memory deficit and in vivo excitatory long-term depression at the hippocampal CA3-CA1 synapses after acute cannabinoids exposure (Han et al., 2012).

Altogether, astroglial alteration in AD and functional changes associated with reactive astrocytes (Smit et al., 2021; Verkhratsky & Nedergaard, 2018) may have a direct impact on synaptic communication (Nanclares et al., 2021) and neuronal network function (Oliveira & Araque, 2022), which eventually would cause brain activity disruption and ultimately cognitive impairment (Escartin et al., 2019; Lines et al., 2022; Smit et al., 2021).

The significant change observed in this study was the increase in microglial CB_1 receptors. The effects of cannabinoids on microglia remain to be deciphered but seem very promising (Esposito et al., 2006; Talarico et al., 2019). Cannabinoids may be beneficial by reducing Aβ aggregation and inhibiting tau hyperphosphorylation as well as ROS generation, among others (Casarejos et al., 2013; Soto-Mercado et al., 2020; Talarico et al., 2019). However, the effect of therapeutic interventions targeting glial cells depends on an adequate balance between attenuation of harmful effects and, at the same time, maintenance of brain function mechanisms (Hansen et al., 2018; Scuderi et al., 2020).

AUTHOR CONTRIBUTIONS

IT, IB-DR, NP, MS, AM, LL, IA-L, LR, IG performed research. IT, IB-DR, NP, IE analyzed data. IE and PG designed research. SRME, CJH, MTG, JR contributed mutant mice. IT, IE, PG wrote the manuscript.

ACKNOWLEDGMENTS

This work was funded by Ministry of Science and Innovation (PID2019-107548RB-I00 to Pedro Grandes; PID2019-108992RB-I00 to Julián Romero), the Basque Government (IT1230-19 and IT1620-22 to Pedro Grandes), and the Research and Education Component of the Advancing a Healthier Wisconsin Endowment at the Medical College of Wisconsin (to Cecilia J. Hillard).

DATA AVAILABILITY STATEMENT

The authors have included full information on the statistical methods and measures used in the present research. Furthermore, the statistical tests applied have been demonstrated to be appropriate in previous papers published by the Grandes laboratory. All raw data used for statistics are available upon request.

ORCID

Cecilia J. Hillard https://orcid.org/0000-0002-9678-748X
Pedro Grandes https://orcid.org/0000-0003-3947-4230

REFERENCES

Abate, G., Uberti, D., & Tambaro, S. (2021). Potential and limits of cannabinoids in Alzheimer's disease therapy. *Biology (Basel)*, *10*(6), 542. https://doi.org/10.3390/biology10060542

Adermark, L., & Bowers, M. S. (2016). Disentangling the role of astrocytes in alcohol use disorder. *Alcoholism: Clinical and Experimental Research*, *40*(9), 1802–1816. https://doi.org/10.1111/acer.13168

Araque, A., Carmignoto, G., Haydon, P. G., Oliet, S. H., Robitaille, R., & Volterra, A. (2014). Gliotransmitters travel in time and space. *Neuron*, *81*(4), 728–739. https://doi.org/10.1016/j.neuron.2014.02.007

Bard, F., Cannon, C., Barbour, R., Burke, R. L., Games, D., Grajeda, H., Guido, T., Hu, K., Huang, J., Johnson-Wood, K., Khan, K., Kholodenko, D., Lee, M., Lieberburg, I., Motter, R., Nguyen, M., Soriano, F., Vasquez, N., Weiss, K., … Yednock, T. (2000). Peripherally administered antibodies against amyloid beta-peptide enter the central nervous system and reduce pathology in a mouse model of Alzheimer disease. *Nature Medicine*, *6*(8), 916–919. https://doi.org/10.1038/78682

Bedse, G., Romano, A., Lavecchia, A. M., Cassano, T., & Gaetani, S. (2015). The role of endocannabinoid signaling in the molecular mechanisms of neurodegeneration in Alzheimer's disease. *Journal of Alzheimer's Disease*, *43*(4), 1115–1136. https://doi.org/10.3233/JAD-141635

Benito, C., Núñez, E., Pazos, M. R., Tolón, R. M., & Romero, J. (2007). The endocannabinoid system and Alzheimer's disease. *Molecular Neurobiology*, *36*(1), 75–81. https://doi.org/10.1007/s12035-007-8006-8

Benito, C., Núñez, E., Tolón, R. M., Carrier, E. J., Rábano, A., Hillard, C. J., & Romero, J. (2003). Cannabinoid CB_2 receptors and fatty acid amide hydrolase are selectively overexpressed in neuritic plaque-associated glia in Alzheimer's disease brains. *Journal of Neuroscience*, *23*(35), 11136–11141. https://doi.org/10.1523/JNEUROSCI.23-35-11136.2003

Beschorner, R., Simon, P., Schauer, N., Mittelbronn, M., Schluesener, H. J., Trautmann, K., Dietz, K., & Meyermann, R. (2007). Reactive astrocytes and activated microglial cells express EAAT1, but not EAAT2, reflecting a neuroprotective potential following ischaemia. *Histopathology*, *50*(7), 897–910. https://doi.org/10.1111/j.1365-2559.2007.02703.x

Bisogno, T., & Di Marzo, V. (2010). Cannabinoid receptors and endocannabinoids: Role in neuroinflammatory and neurodegenerative disorders. *CNS and Neurological Disorders - Drug Targets*, *9*(5), 564–573. https://doi.org/10.2174/187152710793361568

Blasko, I., Stampfer-Kountchev, M., Robatscher, P., Veerhuis, R., Eikelenboom, P., & Grubeck-Loebenstein, B. (2004). How chronic inflammation can affect the brain and support the development of Alzheimer's disease in old age: The role of microglia and astrocytes. *Aging Cell*, *3*(4), 169–176. https://doi.org/10.1111/j.1474-9728.2004.00101.x

Bonilla-Del Río, I., Puente, N., Mimenza, A., Ramos, A., Serrano, M., Lekunberri, L., Gerrikagoitia, I., Christie, B. R., Nahirney, P. C., & Grandes, P. (2021). Acute Δ9-tetrahydrocannabinol prompts rapid changes in cannabinoid CB_1 receptor immunolabeling and subcellular structure in CA1 hippocampus of young adult male mice. *Journal of Comparative Neurology*, *529*(9), 2332–2346. https://doi.org/10.1002/cne.25098

Bonilla-Del Río, I., Puente, N., Peñasco, S., Rico, I., Gutiérrez-Rodríguez, A., Elezgarai, I., Ramos, A., Reguero, L., Gerrikagoitia, I., Christie, B. R., Nahirney, P., & Grandes, P. (2019). Adolescent ethanol intake alters cannabinoid type-1 receptor localization in astrocytes of the adult mouse hippocampus. *Addiction Biology*, *24*(2), 182–192. https://doi.org/10.1111/adb.12585

Bosier, B., Bellocchio, L., Metna-Laurent, M., Soria-Gomez, E., Matias, I., Hebert-Chatelain, E., Cannich, A., Maitre, M., Leste-Lasserre, T., Cardinal, P., Mendizabal-Zubiaga, J., Canduela, M. J., Reguero, L., Hermans, E., Grandes, P., Cota, D., & Marsicano, G. (2013). Astroglial CB_1 cannabinoid receptors regulate leptin signaling in mouse brain astrocytes. *Molecular Metabolism*, *2*(4), 393–404. https://doi.org/10.1016/j.molmet.2013.08.001

Cabral, G. A., & Marciano-Cabral, F. (2005). Cannabinoid receptors in microglia of the central nervous system: Immune functional relevance. *Journal of Leukocyte Biology*, *78*(6), 1192–1197. https://doi.org/10.1189/jlb.0405216

Carlisle, S. J., Marciano-Cabral, F., Staab, A., Ludwick, C., & Cabral, G. A. (2002). Differential expression of the CB_2 cannabinoid receptor by rodent macrophages and macrophage-like cells in relation to cell

activation. *International Immunopharmacology*, *2*(1), 69–82. https://doi.org/10.1016/s1567-5769(01)00147-3

Casarejos, M. J., Perucho, J., Gomez, A., Muñoz, M. P., Fernandez-Estevez, M., Sagredo, O., Fernandez Ruiz, J., Guzman, M., de Yebenes, J. G., & Mena, M. A. (2013). Natural cannabinoids improve dopamine neurotransmission and tau and amyloid pathology in a mouse model of tauopathy. *Journal of Alzheimer's Disease*, *35*(3), 525–539. https://doi.org/10.3233/JAD-130050

Chen, R., Zhang, J., Wu, Y., Wang, D., Feng, G., Tang, Y. P., Chen, C., & Chen, C. (2012). Monoacylglycerol lipase is a therapeutic target for Alzheimer's disease. *Cell Reports*, *2*(5), 1329–1339. https://doi.org/10.1016/j.celrep.2012.09.030

Chung, Y. C., Bok, E., Huh, S. H., Park, J. Y., Yoon, S. H., Kim, S. R., Kim, Y. S., Maeng, S., Park, S. H., & Jin, B. K. (2011). Cannabinoid receptor type 1 protects nigrostriatal dopaminergic neurons against MPTP neurotoxicity by inhibiting microglial activation. *The Journal of Immunology*, *187*(12), 6508–6517. https://doi.org/10.4049/jimmunol.1102435

de Martín, R., Esteban, S., Benito-Cuesta, I., Terradillos, I., Martínez-Relimpio, A. M., Arnanz, M. A., Ruiz-Pérez, G., Korn, C., Raposo, C., Sarott, R. C., Westphal, M. V., Elezgarai, I., Carreira, E. M., Hillard, C. J., Grether, U., Grandes, P., Grande, M. T., & Romero, J. (2022). Cannabinoid CB_2 receptors modulate microglia function and amyloid dynamics in a mouse model of Alzheimer's disease. *Frontiers in Pharmacology*, *13*, 841766. https://doi.org/10.3389/fphar.2022.841766

De Meij, J., Alfanek, Z., Morel, L., Decoeur, F., Leyrolle, Q., Picard, K., Carrier, M., Aubert, A., Séré, A., Lucas, C., Laforest, G., Helbling, J. C., Tremblay, M. E., Cota, D., Moisan, M. P., Marsicano, G., Layé, S., & Nadjar, A. (2021). Microglial cannabinoid type 1 receptor regulates brain inflammation in a sex-specific manner. *Cannabis and Cannabinoid Research*, *6*(6), 488–507. https://doi.org/10.1089/can.2020.0170

Delcambre, G. H., Liu, J., Herrington, J. M., Vallario, K., & Long, M. T. (2016). Immunohistochemistry for the detection of neural and inflammatory cells in equine brain tissue. *PeerJ*, *4*, e1601. https://doi.org/10.7717/peerj.1601

Duffy, S. S., Hayes, J. P., Fiore, N. T., & Moalem-Taylor, G. (2021). The cannabinoid system and microglia in health and disease. *Neuropharmacology*, *190*, 108555. https://doi.org/10.1016/j.neuropharm.2021.108555

Duncan, M., Galic, M. A., Wang, A., Chambers, A. P., McCafferty, D. M., McKay, D. M., Sharkey, K. A., & Pittman, Q. J. (2013). Cannabinoid 1 receptors are critical for the innate immune response to TLR4 stimulation. *American Journal of Physiology-Regulatory, Integrative and Comparative Physiology*, *305*(3), R224–R231. https://doi.org/10.1152/ajpregu.00104.2013

Dzyubenko, E., Gottschling, C., & Faissner, A. (2016). Neuron-glia interactions in neural plasticity: Contributions of neural extracellular matrix and perineuronal nets. *Neural Plasticity*, *2016*, 5214961. https://doi.org/10.1155/2016/5214961

Egaña-Huguet, J., Bonilla-Del Río, I., Gómez-Urquijo, S. M., Mimenza, A., Saumell-Esnaola, M., Borrega-Roman, L., García Del Caño, G., Sallés, J., Puente, N., Gerrikagoitia, I., Elezgarai, I., & Grandes, P. (2021). The absence of the transient receptor potential vanilloid 1 directly impacts on the expression and localization of the endocannabinoid system in the mouse hippocampus. *Frontiers in Neuroscience*, *15*, 645940. https://doi.org/10.3389/fnana.2021.645940

Eljaschewitsch, E., Witting, A., Mawrin, C., Lee, T., Schmidt, P. M., Wolf, S., Hoertnagl, H., Raine, C. S., Schneider-Stock, R., Nitsch, R., & Ullrich, O. (2006). The endocannabinoid anandamide protects neurons during CNS inflammation by induction of MKP-1 in microglial cells. *Neuron*, *49*(1), 67–79. https://doi.org/10.1016/j.neuron.2005.11.027

Escartin, C., Guillemaud, O., & Carrillo-de Sauvage, M. A. (2019). Questions and (some) answers on reactive astrocytes. *Glia*, *67*(12), 2221–2247. https://doi.org/10.1002/glia.23687

Esposito, G., De Filippis, D., Cirillo, C., Sarnelli, G., Cuomo, R., & Iuvone, T. (2006). The astroglial-derived S100beta protein stimulates the expression of nitric oxide synthase in rodent macrophages through p38 MAP kinase activation. *Life Sciences*, *78*(23), 2707–2715. https://doi.org/10.1016/j.lfs.2005.10.023

Facchinetti, F., Del Giudice, E., Furegato, S., Passarotto, M., & Leon, A. (2003). Cannabinoids ablate release of TNFalpha in rat microglial cells stimulated with lypopolysaccharide. *Glia*, *41*(2), 161–168. https://doi.org/10.1002/glia.10177

Farina, C., Aloisi, F., & Meinl, E. (2007). Astrocytes are active players in cerebral innate immunity. *Trends in Immunology*, *28*(3), 138–145. https://doi.org/10.1016/j.it.2007.01.005

Franklin, K. B. J., & Paxinos, G. (2008). *The mouse brain in stereotaxic coordinates. In compact* (3rd ed.). San Diego.

Gomez-Nicola, D., & Perry, V. H. (2015). Microglial dynamics and role in the healthy and diseased brain: A paradigm of functional plasticity. *The Neuroscientist*, *21*(2), 169–184. https://doi.org/10.1177/1073858414530512

Gutiérrez-Rodríguez, A., Bonilla-Del Río, I., Puente, N., Gómez-Urquijo, S. M., Fontaine, C. J., Egaña-Huguet, J., Elezgarai, I., Ruehle, S., Lutz, B., Robin, L. M., Soria-Gómez, E., Bellocchio, L., Padwal, J. D., van der Stelt, M., Mendizabal-Zubiaga, J., Reguero, L., Ramos, A., Gerrikagoitia, I., Marsicano, G., & Grandes, P. (2018). Localization of the cannabinoid type-1 receptor in subcellular astrocyte compartments of mutant mouse hippocampus. *Glia*, *66*(7), 1417–1431. https://doi.org/10.1002/glia.23314

Han, J., Kesner, P., Metna-Laurent, M., Duan, T., Xu, L., Georges, F., Koehl, M., Abrous, D. N., Mendizabal-Zubiaga, J., Grandes, P., Liu, Q., Bai, G., Wang, W., Xiong, L., Ren, W., Marsicano, G., & Zhang, X. (2012). Acute cannabinoids impair working memory through astroglial CB_1 receptor modulation of hippocampal LTD. *Cell*, *148*(5), 1039–1050. https://doi.org/10.1016/j.cell.2012.01.037

Hansen, D. V., Hanson, J. E., & Sheng, M. (2018). Microglia in Alzheimer's disease. *Journal of Cell Biology*, *217*(2), 459–472. https://doi.org/10.1083/jcb.201709069

Haspula, D., & Clark, M. A. (2020). Cannabinoid receptors: An update on cell signaling, pathophysiological roles and therapeutic opportunities in neurological, cardiovascular, and inflammatory diseases. *International Journal of Molecular Sciences*, *21*(20), 7693. https://doi.org/10.3390/ijms21207693

Hu, Q. X., Klatt, G. M., Gudmundsrud, R., Ottestad-Hansen, S., Verbruggen, L., Massie, A., Danbolt, N. C., & Zhou, Y. (2020). Semi-quantitative distribution of excitatory amino acid (glutamate) transporters 1-3 (EAAT1-3) and the cystine-glutamate exchanger (xCT) in the adult murine spinal cord. *Neurochemistry International*, *140*, 104811. https://doi.org/10.1016/j.neuint.2020.104811

Kamphuis, W., Orre, M., Kooijman, L., Dahmen, M., & Hol, E. M. (2012). Differential cell proliferation in the cortex of the APPswePS1dE9 Alzheimer's disease mouse model. *Glia*, *60*(4), 615–629. https://doi.org/10.1002/glia.22295

Kaplan, B. L. (2013). The role of CB_1 in immune modulation by cannabinoids. *Pharmacology & Therapeutics*, *137*(3), 365–374. https://doi.org/10.1016/j.pharmthera.2012.12.004

Kettenmann, H., Hanisch, U. K., Noda, M., & Verkhratsky, A. (2011). Physiology of microglia. *Physiological Reviews*, *91*(2), 461–553. https://doi.org/10.1152/physrev.00011.2010

Klegeris, A., Bissonnette, C. J., & McGeer, P. L. (2003). Reduction of human monocytic cell neurotoxicity and cytokine secretion by ligands of the cannabinoid-type CB_2 receptor. *British J Pharmacology*, *139*(4), 775–786. https://doi.org/10.1038/sj.bjp.0705304

Lehre, K. P., Levy, L. M., Ottersen, O. P., Storm-Mathisen, J., & Danbolt, N. C. (1995). Differential expression of two glial glutamate transporters in the rat brain: Quantitative and immunocytochemical observations. *Journal of Neuroscience*, *15*(3 Pt 1), 1835–1853. https://doi.org/10.1523/JNEUROSCI.15-03-01835.1995

Li, Y., Zhou, Y., & Danbolt, N. C. (2012). The rates of postmortem proteolysis of glutamate transporters differ dramatically between cells and between transporter subtypes. *Journal of Histochemistry & Cytochemistry*, *60*(11), 811–821. https://doi.org/10.1369/0022155412458589

Lines, J., Baraibar, A. M., Fang, C., Martin, E. D., Aguilar, J., Lee, M. K., Araque, A., & Kofuji, P. (2022). Astrocyte-neuronal network interplay is disrupted in Alzheimer's disease mice. *Glia*, *70*(2), 368–378. https://doi.org/10.1002/glia.24112

López, A., Aparicio, N., Pazos, M. R., Grande, M. T., Barreda-Manso, M. A., Benito-Cuesta, I., Vázquez, C., Amores, M., Ruiz-Pérez, G., García-García, E., Beatka, M., Tolón, R. M., Dittel, B. N., Hillard, C. J., & Romero, J. (2018). Cannabinoid CB_2 receptors in the mouse brain: Relevance for Alzheimer's disease. *Journal of Neuroinflammation*, *15*(1), 158. https://doi.org/10.1186/s12974-018-1174-9

Marsicano, G., Wotjak, C. T., Azad, S. C., Bisogno, T., Rammes, G., Cascio, M. G., Hermann, H., Tang, J., Hofmann, C., Zieglgänsberger, W., Di Marzo, V., & Lutz, B. (2002). The endogenous cannabinoid system controls extinction of aversive memories. *Nature*, *418*(6897), 530–534. https://doi.org/10.1038/nature00839

Martín-Moreno, A. M., Reigada, D., Ramírez, B. G., Mechoulam, R., Innamorato, N., Cuadrado, A., & de Ceballos, M. L. (2011). Cannabidiol and other cannabinoids reduce microglial activation in vitro and in vivo: Relevance to Alzheimer's disease. *Molecular Pharmacology*, *79*(6), 964–973. https://doi.org/10.1124/mol.111.071290

McAlpine, C. S., Park, J., Griciuc, A., Kim, E., Choi, S. H., Iwamoto, Y., Kiss, M. G., Christie, K. A., Vinegoni, C., Poller, W. C., Mindur, J. E., Chan, C. T., He, S., Janssen, H., Wong, L. P., Downey, J., Singh, S., Anzai, A., Kahles, F., … Swirski, F. K. (2021). Astrocytic interleukin-3 programs microglia and limits Alzheimer's disease. *Nature*, *595*(7869), 701–706. https://doi.org/10.1038/s41586-021-03734-6

Mecha, M., Carrillo-Salinas, F. J., Feliú, A., Mestre, L., & Guaza, C. (2016). Microglia activation states and cannabinoid system: Therapeutic implications. *Pharmacology & Therapeutics*, *166*, 40–55. https://doi.org/10.1016/j.pharmthera.2016.06.011

Mecha, M., Feliú, A., Carrillo-Salinas, F. J., Rueda-Zubiaurre, A., Ortega-Gutiérrez, S., de Sola, R. G., & Guaza, C. (2015). Endocannabinoids drive the acquisition of an alternative phenotype in microglia. *Brain, Behavior, and Immunity*, *49*, 233–245. https://doi.org/10.1016/j.bbi.2015.06.002

Metna-Laurent, M., & Marsicano, G. (2015). Rising stars: Modulation of brain functions by astroglial type-1 cannabinoid receptors. *Glia*, *63*(3), 353–364. https://doi.org/10.1002/glia.22773

Molina-Holgado, F., Molina-Holgado, E., Guaza, C., & Rothwell, N. J. (2002). Role of CB_1 and CB_2 receptors in the inhibitory effects of cannabinoids on lipopolysaccharide-induced nitric oxide release in astrocyte cultures. *Journal of Neuroscience Research*, *67*(6), 829–836. https://doi.org/10.1002/jnr.10165

Nanclares, C., Baraibar, A. M., Araque, A., & Kofuji, P. (2021). Dysregulation of astrocyte-neuronal communication in Alzheimer's disease. *International Journal of Molecular Sciences*, *22*(15), 7887. https://doi.org/10.3390/ijms22157887

Navarrete, M., & Araque, A. (2008). Endocannabinoids mediate neuron-astrocyte communication. *Neuron*, *57*(6), 883–893. https://doi.org/10.1016/j.neuron.2008.01.029

Navarrete, M., & Araque, A. (2010). Endocannabinoids potentiate synaptic transmission through stimulation of astrocytes. *Neuron*, *68*(1), 113–126. https://doi.org/10.1016/j.neuron.2010.08.043

Navarro, G., Borroto-Escuela, D., Angelats, E., Etayo, Í., Reyes-Resina, I., Pulido-Salgado, M., Rodríguez-Pérez, A. I., Canela, E. I., Saura, J., Lanciego, J. L., Labandeira-García, J. L., Saura, C. A., Fuxe, K., & Franco, R. (2018). Receptor-heteromer mediated regulation of endocannabinoid signaling in activated microglia. Role of CB_1 and CB_2 receptors and relevance for Alzheimer's disease and levodopa-induced dyskinesia. *Brain, Behavior, and Immunity*, *67*, 139–151. https://doi.org/10.1016/j.bbi.2017.08.015

Oakley, H., Cole, S. L., Logan, S., Maus, E., Shao, P., Craft, J., Guillozet-Bongaarts, A., Ohno, M., Disterhoft, J., Van Eldik, L., Berry, R., & Vassar, R. (2006). Intraneuronal β-amyloid aggregates, neurodegeneration, and neuron loss in transgenic mice with five familial Alzheimer's disease mutations: Potential factors in amyloid plaque formation. *Journal of Neuroscience*, *26*(40), 10129–10140. https://doi.org/10.1523/JNEUROSCI.1202-06.2006

Oblak, A. L., Lin, P. B., Kotredes, K. P., Pandey, R. S., Garceau, D., Williams, H. M., Uyar, A., O'Rourke, R., O'Rourke, S., Ingraham, C., Bednarczyk, D., Belanger, M., Cope, Z. A., Little, G. J., Williams, S. G., Ash, C., Bleckert, A., Ragan, T., Logsdon, B. A., … Lamb, B. T. (2021). Comprehensive evaluation of the 5xFAD mouse model for preclinical testing applications: A model-AD study. *Frontiers in Aging Neuroscience*, *13*, 713726. https://doi.org/10.3389/fnagi.2021.713726

Oliveira, J. F., & Araque, A. (2022). Astrocyte regulation of neural circuit activity and network states. *Glia*, *70*(8), 1455–1466. https://doi.org/10.1002/glia.24178

Olmos-Alonso, A., Schetters, S. T., Sri, S., Askew, K., Mancuso, R., Vargas-Caballero, M., Holscher, C., Perry, V. H., & Gomez-Nicola, D. (2016). Pharmacological targeting of CSF1R inhibits microglial proliferation and prevents the progression of Alzheimer's-like pathology. *Brain*, *139*(Pt 3), 891–907. https://doi.org/10.1093/brain/awv379

Puente, N., Bonilla-Del Río, I., Achicallende, S., Nahirney, P. C., & Grandes, P. (2019). High-resolution immunoelectron microscopy techniques for revealing distinct subcellular type 1 cannabinoid receptor domains in brain. *Bio-Protocol*, *9*(2), e3145. https://doi.org/10.21769/BioProtoc.3145

Ramírez, B. G., Blázquez, C., Gómez del Pulgar, T., Guzmán, M., & de Ceballos, M. L. (2005). Prevention of Alzheimer's disease pathology by cannabinoids: Neuroprotection mediated by blockade of microglial activation. *Journal of Neuroscience*, *25*(8), 1904–1913. https://doi.org/10.1523/JNEUROSCI.4540-04.2005

Renau-Piqueras, J., Zaragoza, R., De Paz, P., Baguena-Cervellera, R., Megias, L., & Guerri, C. (1989). Effects of prolonged ethanol exposure on the glial fibrillary acidic protein-containing intermediate filaments of astrocytes in primary culture: A quantitative immunofluorescence and immunogold electron microscopic study. *Journal of Histochemistry & Cytochemistry*, *37*(2), 229–240. https://doi.org/10.1177/37.2.2642942

Ribeiro, R., Yu, F., Wen, J., Vana, A., & Zhang, Y. (2013). Therapeutic potential of a novel cannabinoid agent CB52 in the mouse model of experimental autoimmune encephalomyelitis. *Neuroscience*, *254*, 427–442. https://doi.org/10.1016/j.neuroscience.2013.09.005

Ruiz de Martín Esteban, S., Benito-Cuesta, I., Terradillos, I., Martínez-Relimpio, A. M., Arnanz, M. A., Ruiz-Pérez, G., Korn, C., Raposo, C., Sarott, R. C., Westphal, M. V., Elezgarai, I., Carreira, E. M., Hillard, C. J., Grether, U., Grandes, P., Grande, M. T., & Romero, J. (2022). Cannabinoid CB_2 receptors modulate microglia function and amyloid dynamics in a mouse model of Alzheimer's disease. *Frontiers in Pharmacology*, *13*, 841766. https://doi.org/10.3389/fphar.2022.841766

Schmitt, A., Asan, E., Püschel, B., & Kugler, P. (1997). Cellular and regional distribution of the glutamate transporter GLAST in the CNS of rats: Nonradioactive in situ hybridization and comparative immunocytochemistry. *Journal of Neuroscience*, *17*(1), 1–10. https://doi.org/10.1523/JNEUROSCI.17-01-00001.1997

Scuderi, C., Facchinetti, R., Steardo, L., & Valenza, M. (2020). Neuroinflammation in Alzheimer's disease: Friend or foe? *The FASEB Journal*, *34*(S1), 1. https://doi.org/10.1096/fasebj.2020.34.s1.00381

Sheng, W. S., Hu, S., Min, X., Cabral, G. A., Lokensgard, J. R., & Peterson, P. K. (2005). Synthetic cannabinoid WIN55,212-2 inhibits generation of inflammatory mediators by IL-1beta-stimulated human astrocytes. *Glia*, *49*(2), 211–219. https://doi.org/10.1002/glia.20108

Sinha, D., Bonner, T. I., Bhat, N. R., & Matsuda, L. A. (1998). Expression of the CB_1 cannabinoid receptor in macrophage-like cells from brain tissue: Immunochemical characterization by fusion protein antibodies. *Journal of Neuroimmunology*, *82*(1), 13–21. https://doi.org/10.1016/S0165-5728(97)00181-1

Smit, T., Deshayes, N. A. C., Borchelt, D. R., Kamphuis, W., Middeldorp, J., & Hol, E. M. (2021). Reactive astrocytes as treatment targets in Alzheimer's disease-systematic review of studies using the APPswePS1dE9 mouse model. *Glia*, *69*(8), 1852–1881. https://doi.org/10.1002/glia.23981

Soto-Mercado, V., Mendivil-Perez, M., Velez-Pardo, C., Lopera, F., & Jimenez-Del-Rio, M. (2020). Cholinergic-like neurons carrying PSEN1 E280A mutation from familial Alzheimer's disease reveal intraneuronal sAPPβ fragments accumulation, hyperphosphorylation of TAU, oxidative stress, apoptosis and Ca2+ dysregulation: Therapeutic implications. *PLoS One*, *15*(5), e0221669. https://doi.org/10.1371/journal.pone.0221669

Stefano, G. B., Liu, Y., & Goligorsky, M. S. (1996). Cannabinoid receptors are coupled to nitric oxide release in invertebrate immunocytes, microglia, and human monocytes. *Journal of Biological Chemistry*, *271*(32), 19238–19242. https://doi.org/10.1074/jbc.271.32.19238

Steiner, A. A., Molchanova, A. Y., Dogan, M. D., Patel, S., Pétervári, E., Balaskó, M., Wanner, S. P., Eales, J., Oliveira, D. L., Gavva, N. R., Almeida, M. C., Székely, M., & Romanovsky, A. A. (2011). The hypothermic response to bacterial lipopolysaccharide critically depends on brain CB_1, but not CB_2 or TRPV1, receptors. *Journal of Physiology*, *589*(Pt 9), 2415–2431. https://doi.org/10.1113/jphysiol.2010.202465

Stella, N. (2009). Endocannabinoid signaling in microglial cells. *Neuropharmacology*, *56*(Suppl. 1), 244–253. https://doi.org/10.1016/j.neuropharm.2008.07.037

Stella, N. (2010). Cannabinoid and cannabinoid-like receptors in microglia, astrocytes, and astrocytomas. *Glia*, *58*(9), 1017–1030. https://doi.org/10.1002/glia.20983

Szabo, M., & Gulya, K. (2013). Development of the microglial phenotype in culture. *Neuroscience*, *241*, 280–295. https://doi.org/10.1016/j.neuroscience.2013.03.033

Talarico, G., Trebbastoni, A., Bruno, G., & de Lena, C. (2019). Modulation of the cannabinoid system: A new perspective for the treatment of the Alzheimer's disease. *Current Neuropharmacology*, *17*(2), 176–183. https://doi.org/10.2174/1570159X16666180702144644

Thion, M. S., Low, D., Silvin, A., Chen, J., Grisel, P., Schulte-Schrepping, J., Blecher, R., Ulas, T., Squarzoni, P., Hoeffel, G., Coulpier, F., Siopi, E., David, F. S., Scholz, C., Shihui, F., Lum, J., Amoyo, A. A., Larbi, A., Poidinger, M., … Garel, S. (2018). Microbiome influences prenatal and adult microglia in a sex-specific manner. *Cell*, *172*(3), 500–516.e16. https://doi.org/10.1016/j.cell.2017.11.042

Verkhratsky, A., & Nedergaard, M. (2018). Physiology of astroglia. *Physiological Reviews*, *98*(1), 239–389. https://doi.org/10.1152/physrev.00042.2016

Waksman, Y., Olson, J. M., Carlisle, S. J., & Cabral, G. A. (1999). The central cannabinoid receptor (CB_1) mediates inhibition of nitric oxide production by rat microglial cells. *Journal of Pharmacology and Experimental Therapeutics*, *288*(3), 1357–1366.

Walter, L., Franklin, A., Witting, A., Wade, C., Xie, Y., Kunos, G., Mackie, K., & Stella, N. (2003). Nonpsychotropic cannabinoid receptors regulate microglial cell migration. *Journal of Neuroscience*, *23*(4), 1398–1405. https://doi.org/10.1523/JNEUROSCI.23-04-01398.2003

Wyss-Coray, T., Loike, J. D., Brionne, T. C., Lu, E., Anankov, R., Yan, F., Silverstein, S. C., & Husemann, J. (2003). Adult mouse astrocytes degrade amyloid-beta in vitro and in situ. *Nature Medicine*, *9*(4), 453–457. https://doi.org/10.1038/nm838

How to cite this article: Terradillos, I., Bonilla-Del Río, I., Puente, N., Serrano, M., Mimenza, A., Lekunberri, L., Anaut-Lusar, I., Reguero, L., Gerrikagoitia, I., Ruiz de Martín Esteban, S., Hillard, C. J., Grande, M. T., Romero, J., Elezgarai, I., & Grandes, P. (2023). Altered glial expression of the cannabinoid 1 receptor in the subiculum of a mouse model of Alzheimer's disease. *Glia*, *71*(4), 866–879. https://doi.org/10.1002/glia.24312